

## Study on catalysis by carbonyl cluster-derived SiO<sub>2</sub>-supported rhodium for ethylene hydroformylation

Lin Huang<sup>1</sup>, Yide Xu, Wengui Guo, Anming Liu, Daming Li and Xiexian Guo

*State Key Laboratory of Catalysis, Dalian Institute of Chemical Physics, Chinese Academy of Sciences, PO Box 110, 116023 Dalian, PR China*

Received 11 November 1994; accepted 25 January 1995

Atmospheric hydroformylation of ethylene was studied under differential conditions over Rh<sub>4</sub>(CO)<sub>12</sub>-derived Rh/SiO<sub>2</sub> catalysts. The specific activities as functions of Rh dispersions show that ethylene hydroformylation is structure sensitive and ethylene hydrogenation structure insensitive. These structural dependences and in situ IR observations show that Rh<sup>0</sup> is the unique active site for catalytic ethylene hydroformylation on Rh/SiO<sub>2</sub>. The reactions of Rh<sup>0</sup>-coordinated CO and Rh<sup>0</sup>-adsorbed CO with C<sub>2</sub>H<sub>4</sub> + H<sub>2</sub> at 293 K were monitored by IR spectroscopy. The linear CO adsorbed on Rh<sup>0</sup>/SiO<sub>2</sub> is consumed with formation of propanal, whereas the coordinated CO in Rh<sub>6</sub>(CO)<sub>16</sub>/SiO<sub>2</sub> and its derivative do not participate in CO insertion. IR study of the thermal decomposition of Rh<sub>6</sub>(CO)<sub>16</sub>/SiO<sub>2</sub> indicates that the cluster can be stabilized on the surface up to 548 K by gaseous CO under hydroformylation conditions. Moreover, the Rh<sub>6</sub>(CO)<sub>16</sub>/SiO<sub>2</sub> system exhibits increased catalytic hydroformylation activity with reducing coordinated CO. These results show that coordinative unsaturation on the Rh<sup>0</sup> surface is necessary for heterogeneously rhodium-catalyzed hydroformylation and that totally decarbonylated Rh<sup>0</sup>/SiO<sub>2</sub> is most effective. In addition, the oxidation of Rh<sup>0</sup> by surface OH<sup>-</sup> is discussed.

**Keywords:** Rh<sub>4</sub>(CO)<sub>12</sub>-derived Rh/SiO<sub>2</sub>; surface Rh<sup>0</sup>; Rh<sup>0</sup> oxidation; ethylene hydroformylation; ethylene hydrogenation; structure sensitive; structure insensitive; coordinative unsaturation

### 1. Introduction

In C<sub>1</sub> chemistry, catalytic research on syngas conversion to oxygenated products and hydroformylation is being increasingly developed. The introduction of traditional olefin hydroformylation into heterogeneous catalysis has attracted great interest. Notable advances have been made on the selective synthesis of oxygenates

<sup>1</sup> To whom correspondence should be addressed.

[1–7] and the molecular modeling of CO insertion in Fischer–Tropsch reactions [8–13] on supported transition metal catalysts. Of all the metals, Rh is most frequently studied as the active center grafted on inorganic oxides and zeolites because of its multifunctional activation of CO molecules. A number of papers have been reported to characterize the rhodium active sites in conjunction with mechanistic concepts in the heterogeneous hydroformylation reactions [8–11, 13, 14].

For the molecular approach to heterogeneous catalysts in Fischer–Tropsch synthesis and hydroformylation, organometallic clusters are known as promising precursors of highly dispersed metallic particles and unusual catalytic species. Many examples concerning heterogeneous catalysis by cluster-derived rhodium for olefin hydroformylation have been quoted in the literature [2, 9, 11, 15, 16]. In the present paper, we report an investigation of atmospheric ethylene hydroformylation over SiO<sub>2</sub>-supported rhodium catalysts prepared from Rh<sub>4</sub>(CO)<sub>12</sub>. In an account of the structural effects, we examine the influences of Rh dispersion on catalytic behaviors in hydroformylation and hydrogenation of ethylene. To clarify the nature of the catalytic active site on Rh/SiO<sub>2</sub>, we studied the interactions of Rh with surface OH<sup>−</sup> and the hydroformylation gases in terms of IR data. We also compare the reactivities of coordinated CO and adsorbed CO in CO insertion, and the activities of Rh carbonyls and metallic Rh particles in ethylene hydroformylation by IR study, to understand the contribution of the carbonyl ligand to the catalysis.

## 2. Experimental

Rh<sub>4</sub>(CO)<sub>12</sub> was synthesized as described by Chini and Martinengo [17]. SiO<sub>2</sub> used was a non-porous silica “Aerosil” purchased from Degussa, with a surface area of 200 m<sup>2</sup>/g. *n*-hexane for use as the solvent was distilled over P<sub>2</sub>O<sub>5</sub> and stored under Ar over activated 5 Å molecular sieves. The gases used (H<sub>2</sub>, CO, C<sub>2</sub>H<sub>4</sub>, and Ar) had a purity of 99.99%. Before admission into the reactor and IR cell, they were passed through activated 5 Å molecular sieves and Mn/MnO to eliminate traces of water and oxygen.

Rh<sub>4</sub>(CO)<sub>12</sub> was employed as the starting material to prepare SiO<sub>2</sub>-supported rhodium catalysts. In order to obtain Rh particles as well dispersed as possible on the surface, the supporting SiO<sub>2</sub> (60–80 mesh granule) was predehydroxylated in vacuum ( $1.3 \times 10^{-6}$  kPa) at 673 K for 5 h. Afterwards, it was impregnated with Rh<sub>4</sub>(CO)<sub>12</sub> from *n*-hexane solution under atmospheric Ar using a Schlenk technique. The results of in situ IR monitoring indicate that the initial cluster Rh<sub>4</sub>(CO)<sub>12</sub> is unchanged on SiO<sub>2</sub> thus treated in the presence of *n*-hexane under Ar and it transformed into Rh<sub>6</sub>(CO)<sub>16</sub> upon evacuation of the solvent, as shown in fig. 1 (b) and (c) respectively. So is the case of SiO<sub>2</sub> pretreated at 293 K. The downward shift of bridged carbonyl bands for Rh<sub>4</sub>(CO)<sub>12</sub> in fig. 1 (b) as compared with those in fig. 1 (a), is probably due to the influence of polar environment. A similar shift was noted with a CH<sub>2</sub>Cl<sub>2</sub> solution of Rh<sub>4</sub>(CO)<sub>12</sub> exhibiting the carbonyl bands at

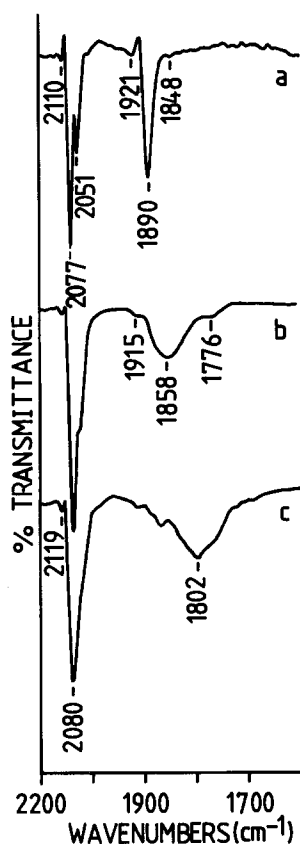


Fig. 1. IR spectra in the  $\nu(\text{CO})$  region of rhodium carbonyl clusters. (a)  $\text{Rh}_4(\text{CO})_{12}$  in *n*-hexane; (b) after 1 h contact of  $\text{SiO}_2$  dehydroxylated at 673 K and the above solution under Ar; (c) after 2 h evacuation ( $1.3 \times 10^{-6}$  kPa), following impregnation of  $\text{SiO}_2$  dehydroxylated at 673 K with  $\text{Rh}_4(\text{CO})_{12}/n$ -hexane.

2101w, 2076s, 2048(sh), 1915w, 1879m and 1811w  $\text{cm}^{-1}$ . The formation of  $\text{Rh}_6(\text{CO})_{16}$  from  $\text{Rh}_4(\text{CO})_{12}$  on  $\text{SiO}_2$  was reported earlier [18]. After removal of the solvent under vacuum, the resulting  $\text{Rh}_6(\text{CO})_{16}/\text{SiO}_2$  samples were transferred to the reactor under Ar.

Atmospheric hydroformylation of ethylene was conducted at 423 K in a glass tubing (i.d. = 7 mm) flow reactor. In each test 0.1 g  $\text{Rh}_6(\text{CO})_{16}/\text{SiO}_2$  sample was charged. The precursors were decarbonylated in flowing  $\text{H}_2$  at 623 K for 2 h, after which  $\text{H}_2$  was replaced by a reaction gas mixture consisting of  $\text{C}_2\text{H}_4$ , CO and  $\text{H}_2$  (1 : 1 : 1 molar ratio, 60 ml/min) at 423–473 K. To keep the reaction under differential conditions, the conversion of  $\text{C}_2\text{H}_4$  was controlled below 10%. Data were taken 5 h after the initiation of reaction. Both hydrocarbons and oxygenates were analyzed on line by gas chromatography, using a 2 m Porapak R column and a flame ionization detector.

IR spectra were measured in Bio-Rad FTS-7 and Hitachi 270-30 spectrophot-

ometers. Each solid sample was compressed into a wafer of 10 mg ( $d = 15$  mm) and placed in a double beam IR cell with CaF<sub>2</sub> windows described in detail previously [19]. The wafer was then subjected to the desired treatments. The IR spectra were recorded at room temperature in the presence of the gas phase, by subtracting the SiO<sub>2</sub> and gaseous contributions.

The metal dispersion was evaluated by H<sub>2</sub> chemisorption stoichiometry measured in a Chemisorb 2800 apparatus, and the H<sub>2</sub>–O<sub>2</sub> titration method of Wanke and Dougharty [20].

The metal contents of the samples studied were determined by X-ray fluorescence spectroscopy.

### 3. Results

#### 3.1. DISPERSION EFFECTS OF SURFACE Rh ON ETHYLENE HYDROFORMYLATION

To search for a correlation between heterogeneous hydroformylation kinetics and the Rh surface structural features, a variety of Rh/SiO<sub>2</sub> catalysts were prepared from Rh<sub>4</sub>(CO)<sub>12</sub> with the Rh content ranging from 0.2 to 5%. Specific catalytic activities to propanal and ethane were determined as a function of Rh content at 423 K.

##### 3.1.1. Dispersion state of Rh on SiO<sub>2</sub>

Four 0.3 g Rh<sub>6</sub>(CO)<sub>16</sub>/SiO<sub>2</sub> samples containing 0.2, 1, 2 and 5% Rh were treated in flowing H<sub>2</sub> at 623 K for 2 h and subsequently evacuated at  $1.3 \times 10^{-6}$  kPa and at 623 K for 10 min before irreversible H<sub>2</sub> adsorption measurements at 293 K. These dispersions are listed in table 1.

In parallel, IR experiments were carried out using CO as a molecular probe to justify distinct metallic surface characters in relation to the amount of Rh depos-

Table 1

Correlation between catalytic properties of Rh/SiO<sub>2</sub> for ethylene hydroformylation<sup>a</sup> and Rh dispersion

%Rh	Dispersion (%)		Activity (mol (Rh mol) <sup>-1</sup> min <sup>-1</sup> )		TOF (min <sup>-1</sup> )				Selectivity to C <sub>2</sub> H <sub>5</sub> CHO (mol%)
	<i>D</i> <sup>b</sup>	<i>D</i> <sup>c</sup>			<i>T</i> <sup>b</sup>		<i>T</i> <sup>c</sup>		
			C <sub>2</sub> H <sub>6</sub>	C <sub>2</sub> H <sub>5</sub> CHO	C <sub>2</sub> H <sub>6</sub>	C <sub>2</sub> H <sub>5</sub> CHO	C <sub>2</sub> H <sub>6</sub>	C <sub>2</sub> H <sub>5</sub> CHO	
0.2	76	49	2.4	5.0	3.2	6.6	4.9	10.2	68
1	41	34	1.4	1.5	3.4	3.7	4.1	4.4	52
2	32	22	1.2	0.9	3.8	2.8	5.5	4.1	43
5	23	17	0.6	0.3	2.6	1.3	3.5	1.8	33

<sup>a</sup> At atmospheric pressure and at 423 K, C<sub>2</sub>H<sub>4</sub> : CO : H<sub>2</sub> = 20 : 20 : 20 ml/min.

<sup>b</sup> Determined by H<sub>2</sub> chemisorption.

<sup>c</sup> Determined by H<sub>2</sub>–O<sub>2</sub> titration.

ited. When H<sub>2</sub> reduced wafers of the four samples were exposed overnight to 3.9 kPa of CO after being evacuated at 293 K or treated by the same procedure as in the H<sub>2</sub> adsorption, the surfaces exhibited a set of regular IR spectra of adsorbed CO shown in fig. 2. Each spectrum consisted of three types of adsorbed CO bands: geminal, linear and bridged. In the case of 0.2% Rh loading, for example, two bands at 2090 and 2026 cm<sup>-1</sup> are assigned to the Rh gem-dicarbonyls, Rh<sup>+</sup>(CO)<sub>2</sub>, and a shoulder at 2055 cm<sup>-1</sup> and a broad band at 1871 cm<sup>-1</sup> are attributed to the linear and bridged CO on Rh<sup>0</sup>. It is noteworthy that the linear CO and bridged CO bands shifted towards lower wavenumbers as the Rh loading decreased, namely as the Rh dispersion increased. Increasing the metal loading resulted in an enhanced intensity ratio of linear CO and bridged CO bands to gem-dicarbonyl bands.

Alternatively, once the same Rh/SiO<sub>2</sub> samples underwent 3 h or longer heating in vacuum at 623 K after H<sub>2</sub> reduction, the adsorption of CO led to another set of

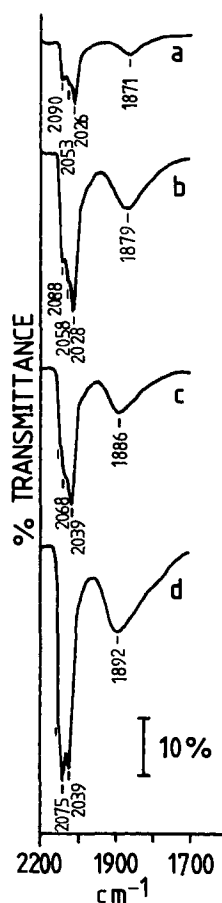


Fig. 2. IR spectra in the  $\nu(\text{CO})$  region of Rh<sub>4</sub>(CO)<sub>12</sub>-derived Rh/SiO<sub>2</sub> under 3.9 kPa of CO for 10 h, after H<sub>2</sub> treatment at 623 K for 2 h and evacuation ( $1.3 \times 10^{-6}$  kPa) at 293 K for 0.5 h. (a) 0.2% Rh; (b) 1% Rh; (c) 2% Rh; (d) 5% Rh.

IR spectra shown in fig. 3. Their shapes were much modified, systematically with an enhanced intensity of gem-dicarbonyl bands with respect to linear CO and bridged CO bands. The linear CO and bridged CO bands disappeared on the Rh/SiO<sub>2</sub> samples with 1% and lower Rh loadings. By contrast, the sample having 5% Rh loading still presented dominant linear CO and bridged CO bands at 2036 and 1856 cm<sup>-1</sup>. An intermediate spectrum of adsorbed CO was obtained with the 2% Rh sample which showed all three types of bands. The intensities of linear CO and bridged CO bands in fig. 3 (c, d) were remarkably smaller than those in fig. 2 (c, d).

### 3.1.2. Influences of Rh dispersion on catalytic performances

The turnover frequency (TOF) which stands for specific catalytic activity here, was determined as a function of Rh content. Table 1 lists the activities and selectivities to propanal and to ethane for catalysts with different Rh content. Regardless of the method used to determine the Rh dispersion, the obtained TOF to propanal increased with decreasing Rh content and, moreover, the selectivity to propanal behaved similarly. In contrast, the TOF to ethane remained substantially unchanged with varying Rh content.

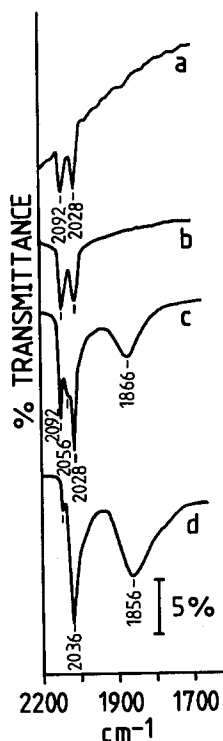


Fig. 3. IR spectra in the  $\nu(\text{CO})$  region of Rh<sub>4</sub>(CO)<sub>12</sub>-derived Rh/SiO<sub>2</sub> under 3.9 kPa of CO for 10 h, after H<sub>2</sub> treatment at 623 K for 2 h and evacuation ( $1.3 \times 10^{-6}$  kPa) at 623 K for 3 h. (a) 0.2% Rh; (b) 1% Rh; (c) 2% Rh; (d) 5% Rh.

### 3.2. IR STUDY RELATED TO THE CATALYTIC ACTIVE SITE

To characterize the Rh species active for the hydroformylation reaction in terms of their valence states and CO adsorption, the gas–solid phase reaction was followed under an in situ atmosphere in the static IR cell by IR spectroscopy shown in fig. 4. A wafer of the catalyst containing 2% Rh freshly derived by H<sub>2</sub> treatment from Rh<sub>6</sub>(CO)<sub>16</sub>/SiO<sub>2</sub> was exposed to an atmospheric mixture of C<sub>2</sub>H<sub>4</sub>, CO and H<sub>2</sub> (1 : 1 : 1 molar ratio). Unlike the case in a CO atmosphere, no gem-dicarbonyl bands appeared and two bands at 2026 and 1896 cm<sup>-1</sup> emerged instead of the surface at 293 K. These two bands are assigned to the adsorbed linear and bridged CO, respectively. The in situ catalytic reaction was left to proceed at 448 K. During a reaction of 3 h, the adsorbed CO spectrum was kept as such without modification. A quite intense band at 1706 cm<sup>-1</sup> and two weak bands at 1446 and 1383 cm<sup>-1</sup> appeared on the surface at the end of reaction, which are assigned to a large amount of propanal and a trace amount of *n*-propanol adsorbed on SiO<sub>2</sub>, which resulted from ethylene hydroformylation.

### 3.3. IR STUDIES ON THE THERMAL DECOMPOSITION OF Rh<sub>6</sub>(CO)<sub>16</sub>/SiO<sub>2</sub> UNDER HYDROFORMYLATION ATMOSPHERES

Based on the IR characterization of the metal catalysts, we were interested in investigating the chemical and catalytic behaviors of the rhodium carbonyl cluster itself supported on SiO<sub>2</sub> under hydroformylation conditions. In order to elucidate

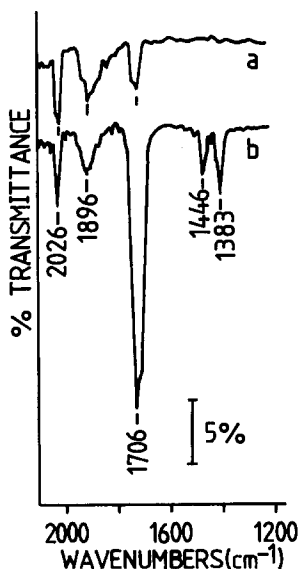


Fig. 4. IR spectra in the  $\nu(\text{CO})$  region of 2% Rh loading Rh<sub>4</sub>(CO)<sub>12</sub>-derived Rh/SiO<sub>2</sub> catalyst after 2 h treatment at 623 K. (a) After 1 h exposure to an atmospheric equimolar mixture of C<sub>2</sub>H<sub>4</sub>, CO and H<sub>2</sub> at 293 K in a static IR cell; (b) after 3 h heating at 448 K following (a).

the contribution of carbonyl species to this catalysis, Rh<sub>6</sub>(CO)<sub>16</sub> was used to simulate surface carbonyl rhodium species since molecular metallic clusters are models of small metallic particles in terms of their geometric and electronic properties [21].

### 3.3.1. Thermal decomposition of Rh<sub>6</sub>(CO)<sub>16</sub>/SiO<sub>2</sub> under C<sub>2</sub>H<sub>4</sub> + CO + H<sub>2</sub>

An equimolar mixture (78 kPa) of C<sub>2</sub>H<sub>4</sub>, CO and H<sub>2</sub> was admitted to a wafer of Rh<sub>6</sub>(CO)<sub>16</sub>/SiO<sub>2</sub> derived from Rh<sub>4</sub>(CO)<sub>12</sub> in the static IR cell. This system was successively thermally treated. Fig. 5 shows IR spectroscopic results taken during this process. According to the spectra after 0.5 h treatments at 378 K and at 403 K, there was no evolution of the cluster features. At the same time, a band at 1706 cm<sup>-1</sup> corresponding to propanal appeared with very weak intensity. The band intensity increased progressively along with temperature as shown in the following spectra. Unexpectedly, there was no concomitant intensity depletion of the bands characteristic of Rh<sub>6</sub>(CO)<sub>16</sub> up to 548 K. This indicates that the supported cluster is able to maintain its integrity under the reaction gases at this stage. At 578 K, intensity weakening of the Rh<sub>6</sub>(CO)<sub>16</sub> bands was observed, accompanying the appearance of two small bands at 2044 and 1863 cm<sup>-1</sup> which are due to the linear and bridged carbonyls on Rh<sup>0</sup>. This shows that the cluster started to transform into metallic aggregates by decarbonylation. When the temperature was raised to 603 K, the decarbonylation of Rh<sub>6</sub>(CO)<sub>16</sub> was nearly complete.

During the above thermal decomposition of Rh<sub>6</sub>(CO)<sub>16</sub>/SiO<sub>2</sub>, the spectral evolution in gas phase in the 3300–2800 cm<sup>-1</sup> region should be noticed. After 3 h treatment at 443 K, the ethylene spectrum decreased slightly in intensity with no observable emergence of the ethane bands. This is probably due to the fairly selective hydroformylation of ethylene. At higher temperatures, the marked observation of the ethane bands at 3012, 2966, 2930 and 2889 cm<sup>-1</sup> which are superimposed with the ethylene bands, is attributed to ethylene hydrogenation in competition with ethylene hydroformylation. It was estimated that the consumption of ethylene was approximately 20% by the end of treatment at 578 K and 30% by the end of treatment at 603 K, mostly due to ethylene hydrogenation. It follows that the majority of the initial gas mixture was kept intact throughout this heat treatment of Rh<sub>6</sub>(CO)<sub>16</sub>/SiO<sub>2</sub> under C<sub>2</sub>H<sub>4</sub> + CO + H<sub>2</sub>.

### 3.3.2. Thermal decomposition of Rh<sub>6</sub>(CO)<sub>16</sub>/SiO<sub>2</sub> under vacuum, H<sub>2</sub>, C<sub>2</sub>H<sub>4</sub> and CO

For the purpose of understanding the stabilizing role of the reaction gases on Rh<sub>6</sub>(CO)<sub>16</sub>/SiO<sub>2</sub> as described above, the thermal decomposition of the supported cluster under vacuum (1.3 × 10<sup>-3</sup> kPa), H<sub>2</sub> (39 kPa), C<sub>2</sub>H<sub>4</sub> (26 kPa) and CO (26 kPa) respectively, was likewise monitored by IR spectroscopy.

As indicated in fig. 6, the supported cluster presented ill thermal stability under vacuum, H<sub>2</sub> and C<sub>2</sub>H<sub>4</sub>. It remarkably decomposed around 373 K in each case to metallic Rh particles covered with coordinated CO, which showed linear and bridged bands towards 2026 and 1868 cm<sup>-1</sup> (fig. 6 (e)). The 2082 cm<sup>-1</sup> band is due



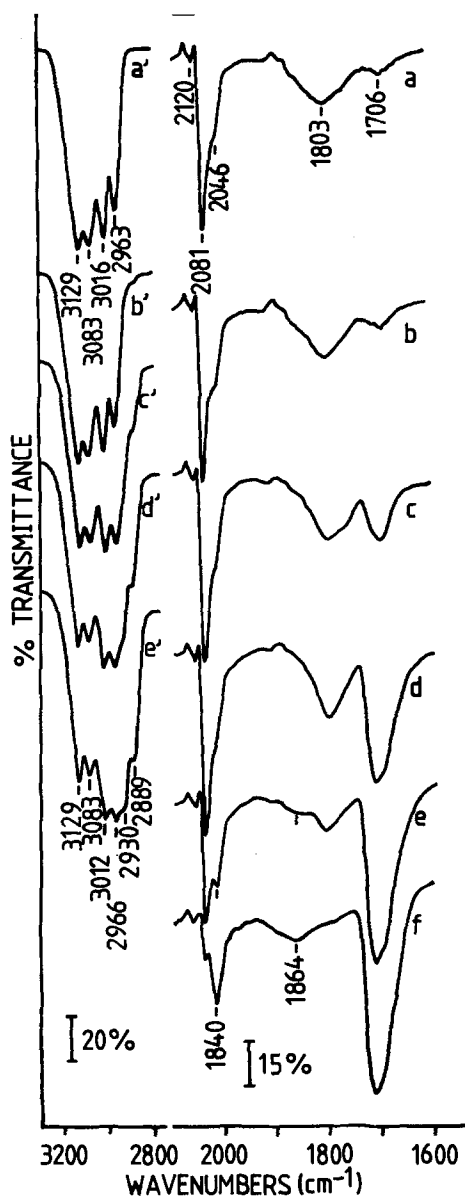


Fig. 5. IR spectra after consecutive thermal treatment of Rh<sub>6</sub>(CO)<sub>16</sub>/SiO<sub>2</sub> under an equimolar mixture of C<sub>2</sub>H<sub>4</sub>, CO and H<sub>2</sub> (total pressure: 78 kPa) in a static IR cell. Surface: (a) 378 K for 0.5 h; (b) 403 K for 0.5 h; (c) 443 K for 3 h; (d) 548 K for 3 h; (e) 578 K for 3 h; (f) 603 K for 3 h. Gas phase: (a') 293 K for 2 h; (b') corresponding to (c); (c') corresponding to (d); (d') corresponding to (e); (e') corresponding to (f).

to Rh<sub>6</sub>(CO)<sub>16</sub> which was not consumed. The decomposition was total below 423 K. A similar thermal instability of Rh<sub>6</sub>(CO)<sub>16</sub>/SiO<sub>2</sub> under vacuum and H<sub>2</sub> was reported earlier by Bilhou et al. [22].

Fig. 7 shows IR monitoring results during thermal decomposition of Rh<sub>6</sub>(CO)<sub>16</sub>

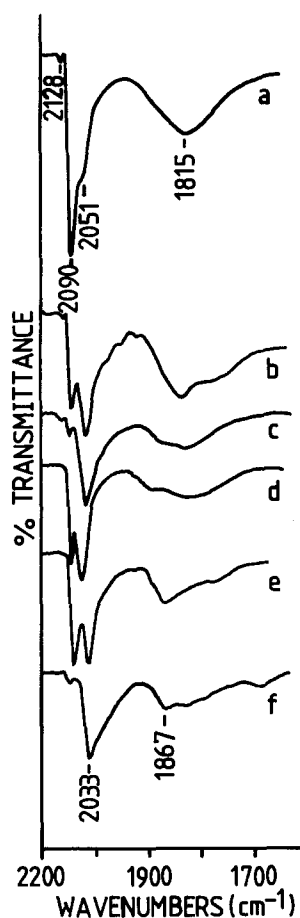


Fig. 6. Surface IR spectra in the  $\nu(\text{CO})$  region after thermal treatment of  $\text{Rh}_6(\text{CO})_{16}/\text{SiO}_2$ . (a) Under vacuum ( $1.3 \times 10^{-6}$  kPa) at 298 K for 2 h; (b) under vacuum ( $1.3 \times 10^{-3}$  kPa) at 378 K for 20 min; (c) at 398 K for 15 min following (b); (d) under  $\text{H}_2$  (39 kPa) at 398 K for 0.5 h; (e) under  $\text{C}_2\text{H}_4$  (26 kPa) at 382 K for 0.5 h; (f) at 409 K for 0.5 h following (e).

/SiO<sub>2</sub> under CO. Up to 545 K, the supported cluster was still well stable under CO, judging from the relative intensities of the  $\text{Rh}_6(\text{CO})_{16}$  bands with varying temperature. When the temperature reached 583 K, two bands at 2062 and 1882  $\text{cm}^{-1}$ , which are assigned to the linear and bridged carbonyls on  $\text{Rh}^0$ , appeared with decreasing  $\text{Rh}_6(\text{CO})_{16}$  band intensity. This indicates that Rh aggregates started to form at the expense of the cluster around this temperature.

### 3.4. IR STUDIES ON THE ACTIVITIES OF SURFACE CO SPECIES FOR HYDROFORMYLATION

#### 3.4.1. Reactivities of surface CO in CO insertion

To clarify the category of CO held on  $\text{Rh}^0$  which is able to participate in hydro-

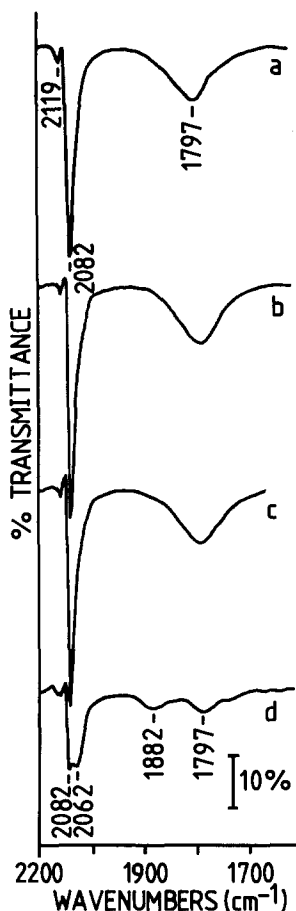


Fig. 7. Surface IR spectra in the  $\nu(\text{CO})$  region after consecutive thermal treatment of  $\text{Rh}_6(\text{CO})_{16}/\text{SiO}_2$  under CO (26 kPa). (a) At 293 K for 10 min; (b) at 498 K for 3 h; (c) at 545 K for 3 h; (d) at 583 K for 2.5 h.

formylation, stoichiometric reactions of  $\text{SiO}_2$ -supported  $\text{Rh}^0$ -coordinated CO and  $\text{Rh}^0$ -adsorbed CO with an equimolar mixture of  $\text{C}_2\text{H}_4$  and  $\text{H}_2$  (total pressure: 52 kPa) were conducted at 293 K in a static IR cell.

Fig. 8 shows IR monitoring results involving the reactions. After 1 h exposure of  $\text{Rh}_6(\text{CO})_{16}/\text{SiO}_2$  to  $\text{C}_2\text{H}_4 + \text{H}_2$ , the  $\text{Rh}_6(\text{CO})_{16}$  spectrum was almost unchanged in intensity. Meanwhile two small bands at 1864 and 1705  $\text{cm}^{-1}$  appeared, corresponding to the bridged carbonyl on  $\text{Rh}^0$  and propanal adsorbed on  $\text{SiO}_2$ . The presence of  $\text{C}_2\text{H}_6$  bands in the gas phase (fig. 8 (b')) suggests that facile ethylene hydrogenation proceeded on a small amount of metallic Rh particles which coexisted with the carbonyl cluster.

To obtain a  $\text{Rh}_6(\text{CO})_{16}$ -derived  $\text{Rh}^0$ -coordinated CO sample, a  $\text{Rh}_6(\text{CO})_{16}/\text{SiO}_2$  wafer was heated under vacuum ( $1.3 \times 10^{-3}$  kPa) at 383 K for 0.5 h. The resulting Rh carbonyls whose IR bands are displayed in fig. 8 (c), did not react

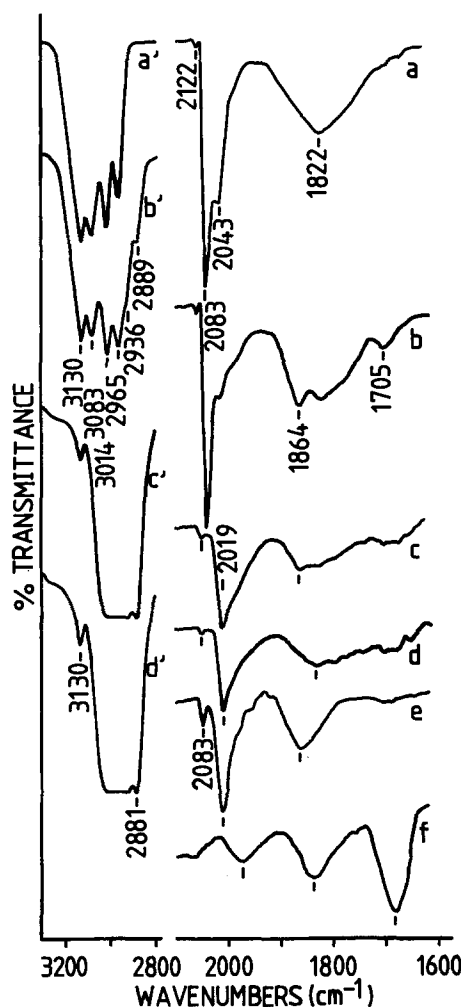


Fig. 8. IR spectra before and after reactions of surface CO species with an equimolar mixture of C<sub>2</sub>H<sub>4</sub> + H<sub>2</sub> (total pressure: 52 kPa) at 293 K in a static IR cell. Surface: (a) Rh<sub>6</sub>(CO)<sub>16</sub>/SiO<sub>2</sub> under vacuum; (b) 1 h exposure to the mixture following (a); (c) after 0.5 h heating of Rh<sub>6</sub>(CO)<sub>16</sub>/SiO<sub>2</sub> under vacuum ( $1.3 \times 10^{-3}$  kPa) at 383 K; (d) 1 h exposure to the mixture following (c); (e) CO adsorbed on Rh<sub>4</sub>(CO)<sub>12</sub>-derived Rh/SiO<sub>2</sub> after H<sub>2</sub> treatment at 623 K; (f) 1 h exposure to the mixture following (e). Gas phase: (a') The initial C<sub>2</sub>H<sub>4</sub> + H<sub>2</sub>; (b') corresponding to (b); (c') corresponding to (d); (d') corresponding to (f).

noticeably with C<sub>2</sub>H<sub>4</sub> + H<sub>2</sub> after 1 h exposure as indicated in fig. 8 (d). However, there was a large formation of ethane at the expense of ethylene in gas phase as shown in fig. 8 (c'), suggesting the presence of a large number of unsaturated Rh<sup>0</sup> centers in this case. At this stage, approximately 20% of the initial gas mixture remained in the system.

In investigating the reactivity of Rh<sup>0</sup>-adsorbed CO in CO insertion, the Rh<sub>6</sub>(CO)<sub>16</sub>/SiO<sub>2</sub> precursor was first decarbonylated in flowing H<sub>2</sub> at 623 K. Then

the resulting Rh/SiO<sub>2</sub> was exposed to 3.9 kPa of CO at 293 K, so that the linear and bridged CO were dominantly formed. Contrary to the cases of Rh<sub>6</sub>(CO)<sub>16</sub>/SiO<sub>2</sub> and its carbonyl derivative, 1 h reaction between the adsorbed CO and C<sub>2</sub>H<sub>4</sub> + H<sub>2</sub> resulted in a sharp band of propanal on the surface, with a strong decrease of the linear CO band intensity (fig. 8 (f)). In the meantime, ethylene hydrogenation occurred rapidly with the consumption of most of the ethylene.

### 3.4.2. Catalytic activities of surface CO species

To reveal the influence of coordinative saturation on Rh<sup>0</sup> on hydroformylation, catalytic ethylene hydroformylations with the three CO species mentioned above were conducted in the static IR cell.

Fig. 9 shows surface IR information about the catalytic system at 378 K after 0.5 h. A wafer of Rh<sub>6</sub>(CO)<sub>16</sub>/SiO<sub>2</sub> was little active as stated hereinbefore. This wafer was then treated under vacuum ( $1.3 \times 10^{-3}$  kPa) at 368 K for 20 min to produce the zerovalent Rh carbonyls which were characterized by the 2046 and 1840 cm<sup>-1</sup> bands. The latter led to an obvious propanal band under catalytic conditions. After the same wafer had completely been decarbonylated under H<sub>2</sub> at 623 K, it exhibited a more intense propanal band under catalytic conditions.

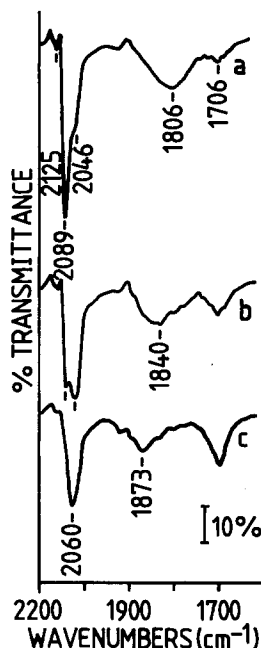


Fig. 9. Surface IR spectra in the  $\nu(\text{CO})$  region after 0.5 h ethylene hydroformylation with surface CO species under an equimolar mixture of C<sub>2</sub>H<sub>4</sub>, CO and H<sub>2</sub> (total pressure: 78 kPa) at 378 K in a static IR cell. (a) Rh<sub>6</sub>(CO)<sub>16</sub>/SiO<sub>2</sub>; (b) a carbonyl Rh catalyst obtained from 20 min treatment of the above precursor wafer under vacuum at 368 K; (c) Rh/SiO<sub>2</sub> obtained from 2 h H<sub>2</sub> treatment of the same wafer following (b).

Fig. 10 shows the similar IR results with another wafer of Rh<sub>6</sub>(CO)<sub>16</sub>/SiO<sub>2</sub> for the hydroformylation at 418 K. The marked difference in catalytic formation of propanal among the three CO species was observed. Since the catalytic activity increased with decreasing amount of coordinated CO, it was suggested that the production of propanal on the Rh<sub>6</sub>(CO)<sub>16</sub>/SiO<sub>2</sub> wafer is ascribed to a small amount of coexisting Rh particles from decomposition of Rh<sub>6</sub>(CO)<sub>16</sub> and that the saturated Rh carbonyls are inactive for hydroformylation.

## 4. Discussion

### 4.1. CHARACTERIZATION OF Rh INTERACTIONS WITH THE SiO<sub>2</sub> SURFACE AND CO BY IR

It is recognized that Rh atoms supported on SiO<sub>2</sub> and Al<sub>2</sub>O<sub>3</sub>, even after H<sub>2</sub> treatment, generally give rise to three types of surface adspecies including Rh gem-dicarbonyls, Rh-adsorbed linear CO and Rh-adsorbed bridged CO under a CO

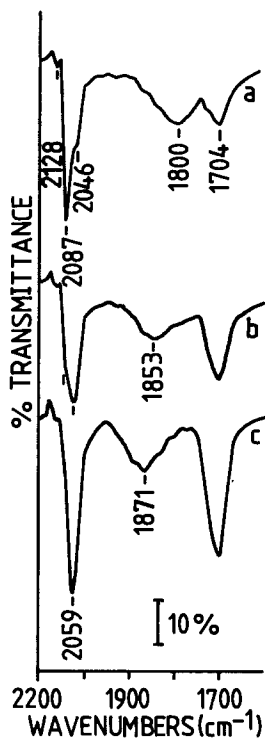
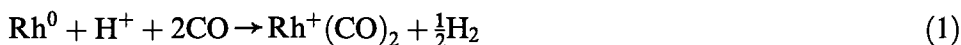


Fig. 10. Surface IR spectra in the  $\nu(\text{CO})$  region after 0.5 h ethylene hydroformylation with surface CO species under an equimolar mixture of C<sub>2</sub>H<sub>4</sub>, CO and H<sub>2</sub> (total pressure: 78 kPa) at 418 K in a static IR cell. (a) Rh<sub>6</sub>(CO)<sub>16</sub>/SiO<sub>2</sub>; (b) a carbonyl Rh catalyst obtained from 0.5 h treatment of the above precursor wafer under vacuum at 368 K; (c) Rh/SiO<sub>2</sub> obtained from 2 h H<sub>2</sub> treatment of the same wafer following (b).

atmosphere. In virtue of our IR results of CO adsorption on the Rh<sub>4</sub>(CO)<sub>12</sub> or Rh<sub>6</sub>(CO)<sub>16</sub> cluster-derived Rh/SiO<sub>2</sub> with Rh loadings below 5%, the Rh surface, even though its loading is as low as 0.2%, gives rise to a mixture of the three adspecies in the common case as shown in fig. 2. This complex CO adsorption has also been observed on Rh/SiO<sub>2</sub> by other authors [10,13]. Combining the measurements of H<sub>2</sub> chemisorption with the IR observations of CO adsorption, it can be deduced that decreasing Rh loading clearly results in the increase of Rh dispersion and the enhancement of the Rh gem-dicarbonyls.

Concerning the formation of surface Rh<sup>+</sup>(CO)<sub>2</sub>, ambiguity and debate exist in the previous studies. Based on IR observations with Rh/Al<sub>2</sub>O<sub>3</sub>, earlier investigators have proposed respectively that a dissociative CO adsorption causes the disruption of the Rh–Rh bond followed by the oxidation of isolated Rh<sup>0</sup> atoms [23], and that protons present as OH<sup>−</sup> on the surface oxidize Rh<sup>0</sup> atoms [24,25]. Recently, Gelin et al. communicated IR isotopic evidence for a dissociative CO adsorption over Rh particles supported on zeolite Y, which favors the mechanism of formation of Rh<sup>+</sup> sites through CO adsorption [26]. Wong et al. demonstrated that the oxidation of Rh<sup>0</sup> to Rh<sup>+</sup> in zeolite NaY occurs favorably by the combined action of H<sup>+</sup> and CO as follows [27]:



In addition, they suggested that the following equilibria are established between Rh ions, Rh metal, H<sup>+</sup> and H<sub>2</sub> [27,28]:



In the present study, the extent to which metallic Rh particles are oxidized to Rh<sup>+</sup> ions on a partially dehydroxylated SiO<sub>2</sub>, was found to be associated with Rh dispersion. More dispersed metal atoms are more easily oxidized, according to the intensity ratios of gem-dicarbonyl bands to Rh<sup>0</sup>-adsorbed CO bands in fig. 2. The oxidation is incomplete on SiO<sub>2</sub> as compared with that on Al<sub>2</sub>O<sub>3</sub>. Nevertheless, it is unclear whether CO serving as an IR probe is instrumental in the oxidation. Our further IR data provide evidence in favor of the oxidative pathway of highly dispersed Rh by the surface OH<sup>−</sup> or H<sup>+</sup> groups. In fact, after the freshly H<sub>2</sub> reduced Rh/SiO<sub>2</sub> samples are treated under vacuum at 623 K for 3 h, the Rh atoms eventually have undergone strong interaction with the acidic OH<sup>−</sup> groups on the surface, which can effectively give rise to Rh<sup>+</sup> sites,



This will produce much more atomically dispersed Rh<sup>+</sup> sites than with a temperature of 293 K. As a consequence, a largely enhanced intensity of gem-dicarbonyl bands relative to linear CO and bridged CO bands was observed in fig. 3. Especially on the surfaces of less than 1% Rh loadings, the Rh<sup>0</sup> atoms seem to convert com-

pletely to Rh<sup>+</sup> ions after interacting with OH<sup>-</sup> groups, the spectra showing only doublet features under CO. Comparing the two sets of IR spectra in figs. 2 and 3, we infer that the direct oxidation of Rh<sup>0</sup> by the surface OH<sup>-</sup> plays a key role in the formation of Rh<sup>+</sup>(CO)<sub>2</sub> since the proportion of the latter increases with increasing oxidizability of OH<sup>-</sup> at a given Rh loading. Here it is worth recalling that only Rh<sup>+</sup>(CO)<sub>2</sub> is formed under CO on reduced Rh/Al<sub>2</sub>O<sub>3</sub> at 2.2% Rh loading [25]. That means that the surface OH<sup>-</sup> of Al<sub>2</sub>O<sub>3</sub> is a strong oxidant as compared with that of SiO<sub>2</sub>. In contrast, the interaction of CO with highly dispersed SiO<sub>2</sub>-supported Rh fails to lead to appreciable formation of Rh<sup>+</sup>(CO)<sub>2</sub> within an enough long time as seen in fig. 2 (a). Moreover, the amount of Rh<sup>+</sup>(CO)<sub>2</sub> on Rh/SiO<sub>2</sub> develops only to a small extent with increasing CO pressure [13,24]. Hence, the Rh<sup>0</sup> → Rh<sup>+</sup> transition is highly dependent on the oxidizability of surface OH<sup>-</sup>, and appears little dependent on CO adsorption in the presence of both surface OH<sup>-</sup> and gaseous CO. We suggest that the interaction mechanism of Rh<sup>0</sup> with surface OH<sup>-</sup> and CO involves the oxidation of Rh<sup>0</sup> to Rh<sup>+</sup> by surface OH<sup>-</sup> before CO coordination to form Rh<sup>+</sup>(CO)<sub>2</sub>.

As for the effect of Rh dispersion on this oxidation, it is seen from figs. 1 and 2 that increasing Rh dispersion is beneficial to the Rh<sup>0</sup> → Rh<sup>+</sup> conversion. A possible explanation for this is that the surface → metallic particle interaction is restricted to their interface only and the number of OH<sup>-</sup> groups around a Rh particle is limited and cannot oxidize all the Rh atoms. Whether the metal atoms in a particle can be completely transformed into isolated ions grafted on the surface, depends on the particle size and the number of surface OH<sup>-</sup> available. The dehydroxylation of SiO<sub>2</sub> at 673 K still leaves a large number of OH<sup>-</sup> groups on the surface [29].

#### 4.2. Rh/SiO<sub>2</sub>-CATALYZED ETHYLENE HYDROFORMYLATION

The dependence of C<sub>1</sub> and hydrocarbon catalytic reactions on surface structural factors is an unsolved question in heterogeneous catalysis. The average metallic particle size statistically determines the proportion of metal atoms in different geometries: face, edge and corner. Previous works have shown the basic relation between metal dispersion, metallic particle size and the geometric feature [30,31]. This relation can also be accounted for by the IR bands of CO adsorbed on Rh in our case. With an increase of Rh dispersion, namely with a decrease of Rh particle size, the downward shifts of linear CO and bridged CO bands can be clearly discerned as shown in fig. 2. This observation signifies that the fraction of edge and corner atoms increases with increase of Rh dispersion [32].

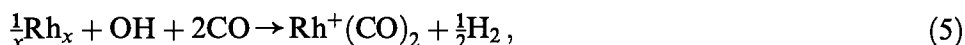
Since the TOF for propanal formation increases with increasing Rh dispersion over the catalysts studied, we suggest that ethylene hydroformylation is structure sensitive. In contrast, the TOF for ethane formation is almost independent of Rh dispersion. We suggest that ethylene hydrogenation is structure insensitive.

The above relationships between TOF and metallic Rh particle size seem to reveal also the characteristics of heterogeneous hydroformylation and hydrogenation.



It should be mentioned that ethylene hydrogenation is said to be a representative structure insensitive reaction, according to the kinetic studies on crystal surfaces at atmospheric pressure as well as at low pressure by Somorjai et al. [33,34]. Its kinetics (rate, activation energies) are the same on crystal surfaces, dispersed particles, films and metal foils [33]. For ethylene hydroformylation, our finding is consistent with the argument of Konishi et al. who proposed that protruding corner atoms are most active for hydroformylation on Rh/SiO<sub>2</sub> [10].

Concerning the nature of hydroformylation active sites on supported Rh, previous works postulated that the electronic states of Pd and Rh active for CO insertion are 1+ [35–38]. On the other hand, reduced Rh/SiO<sub>2</sub> was reported to produce Rh<sup>0</sup> sites which are responsible for CO dissociation and thus hydrocarbon formation [38]. In this work, although the Rh/SiO<sub>2</sub> catalysts yield some Rh<sup>+</sup>(CO)<sub>2</sub> in the CO atmosphere, they display only Rh<sup>0</sup>-adsorbed CO bands under a mixture of C<sub>2</sub>H<sub>4</sub>, CO and H<sub>2</sub>. Basu et al. have assumed not only the involvement of surface OH<sup>−</sup> groups in the disruptive oxidation of Rh<sub>x</sub> crystallites to produce Rh<sup>+</sup>(CO)<sub>2</sub> in eq. (5),



but also its inverse reaction. They provided IR evidence for the inverse reaction on Al<sub>2</sub>O<sub>3</sub> and SiO<sub>2</sub> that the intensities of linear CO and isolated OH<sup>−</sup> bands increased at the expense of those of gem-dicarbonyl bands, while the Rh<sup>+</sup>(CO)<sub>2</sub> species were converted back to Rh<sub>x</sub> species with H<sub>2</sub> treatment. The analogous explanation can be made for our case with coexisting gaseous CO and H<sub>2</sub>. As long as H<sub>2</sub> takes part in the chemisorption on Rh/SiO<sub>2</sub>, the oxidation addition of surface OH<sup>−</sup> to Rh<sup>0</sup> is quenched. Virtually in agreement with the involvement of H<sup>+</sup> in the oxidation and the interconversion between Rh<sup>0</sup> and Rh<sup>+</sup> [28], the admission of H<sub>2</sub> enables the equilibrium (3) to shift to the right. Thus the catalytic hydroformylation active site is likely to be Rh<sup>0</sup> instead of Rh<sup>+</sup>.

Insomuch as H<sub>2</sub> is capable of preventing the oxidation of metallic Rh particles on the surface, the Rh/SiO<sub>2</sub> catalysts pretreated with H<sub>2</sub> should present all its surface Rh atoms available as active sites under a hydroformylation atmosphere. The metallic Rh dispersion measured by H<sub>2</sub> chemisorption can represent reasonably the number of hydroformylation active sites in calculating the TOF.

Actually, the view of zerovalent rhodium as the heterogeneous hydroformylation active site has also been claimed by other groups recently. Arakawa et al., by catalytic and in situ IR studies, showed that ethylene hydroformylation proceeds comparably over SiO<sub>2</sub>-supported highly dispersed Rh particles and a SiO<sub>2</sub>-supported HRh(CO)(PPh<sub>3</sub>)<sub>3</sub> complex [39]. Takahashi et al., who studied the zeolite Y-supported rhodium system by means of IR and XPS, indicated that the catalytic activity for ethylene hydroformylation can be considerably enhanced only when Rh<sup>+</sup>(CO)<sub>2</sub> is reduced with H<sub>2</sub> to metallic Rh particles [14]. A detailed research by Chuang and Pien on Rh/SiO<sub>2</sub> catalysts treated in different conditions using IR

spectroscopy demonstrated that the linear CO adsorbed on both Rh<sup>0</sup> and Rh<sup>+</sup> sites participates in CO insertion leading to the formation of propanal from C<sub>2</sub>H<sub>4</sub> and H<sub>2</sub>. By contrast, Rh<sup>+</sup>(CO)<sub>2</sub> has proven to be inactive for hydroformylation on zeolite Y [14] and SiO<sub>2</sub> [13], since the geminal CO do not participate in CO insertion. Although the Rh<sup>+</sup> site can become active once having linear CO adsorbed on it, reduced Rh/SiO<sub>2</sub> catalysts cannot give Rh<sup>+</sup> species except Rh<sup>0</sup>-adsorbed linear and bridged CO under catalytic hydroformylation conditions, following Chuang and Pien and our work. Even in the cases of oxidized and sulfided Rh/SiO<sub>2</sub>, complete reduction of surface Rh<sup>+</sup> is easy under moderate catalytic conditions [13]. Accordingly, Rh<sup>0</sup> is actually the unique active site for hydroformylation and concomitant hydrogenation on the Rh/SiO<sub>2</sub> catalysts.

#### 4.3. CATALYSIS BY SiO<sub>2</sub>-SUPPORTED Rh CARBONYLS

The behaviors of Rh<sub>6</sub>(CO)<sub>16</sub>/SiO<sub>2</sub> and its carbonyl derivative under ethylene hydroformylation conditions were shown in terms of IR data in this study. First, Rh<sub>6</sub>(CO)<sub>16</sub> can be well stabilized on SiO<sub>2</sub> (till 548 K) under a hydroformylation atmosphere. This stabilization is explicitly ascribed to CO in the gas mixture, as Rh<sub>6</sub>(CO)<sub>16</sub>/SiO<sub>2</sub> displays as good a thermal stability only under CO as under the gas mixture. Subsequently, the cluster starts to decompose to metallic Rh particles covered with CO from 548 K. Since no gem-dicarbonyl bands appear in fig. 5, the original zerovalent state of rhodium in the Rh<sub>6</sub>(CO)<sub>16</sub> cluster remains unchanged throughout the thermal decomposition. This observation is further evidence that the oxidation of Rh<sup>0</sup> by surface OH<sup>-</sup> is inhibited in the presence of H<sub>2</sub> and that Rh<sup>0</sup> is uniquely responsible for hydroformylation. Consequently, it is evident that the (CO + H<sub>2</sub>)-containing gas mixture is able to stabilize supported rhodium carbonyl clusters on the one hand, and prevent the oxidation of Rh<sup>0</sup> on the surface on the other hand.

Simultaneously, it is highly likely that Rh<sub>6</sub>(CO)<sub>16</sub>/SiO<sub>2</sub> is inactive itself for hydroformylation. As a matter of fact, no propanal band was present together with those of Rh<sub>6</sub>(CO)<sub>16</sub> under catalytic conditions at temperatures lower than 378 K. However, at 378 K the carbonyl and non-carbonyl metallic Rh particles derived from Rh<sub>6</sub>(CO)<sub>16</sub> clearly give rise to propanal as evidenced by IR in fig. 9. More decarbonylated species is more active (figs. 9 and 10). These results seem to show that the active site Rh<sup>0</sup> must be coordinatively unsaturated and the catalytic activity increases with increasing unsaturation, and that the Rh<sup>0</sup>-coordinated CO does not act in the CO insertion step. Indeed, different unsaturations on Rh<sup>0</sup> can be detected in that ethylene hydrogenation results in a small amount of ethane on the Rh<sub>6</sub>(CO)<sub>16</sub>/SiO<sub>2</sub> sample, and an appreciable amount of ethane on the carbonyl and non-carbonyl Rh<sup>0</sup> sites derived from Rh<sub>6</sub>(CO)<sub>16</sub>, as shown in fig. 8. The study of reactivities of Rh carbonyls with C<sub>2</sub>H<sub>4</sub> + H<sub>2</sub> proves that coordinated CO in Rh<sub>6</sub>(CO)<sub>16</sub>/SiO<sub>2</sub> and its carbonyl derivative only participates with difficulty in CO

insertion as compared with the Rh<sup>0</sup>-adsorbed CO. The inactivity of Rh<sub>6</sub>(CO)<sub>16</sub> for hydroformylation has been reported on zeolite Y by Rode and Takahashi et al. [40,14].

But for the observation of the propanal band at 1706 cm<sup>-1</sup> appearing together with the Rh<sub>6</sub>(CO)<sub>16</sub> spectrum under the ethylene hydroformylation atmosphere above 378 K, we assume that this may be due to a small minority of metallic Rh particles or/and unsaturated Rh carbonyls arising from decomposition of the cluster. They might be formed during exposure of Rh<sub>6</sub>(CO)<sub>16</sub>/SiO<sub>2</sub> to the reaction gas mixture [14]. The reproducible results of the C<sub>2</sub>H<sub>4</sub> + H<sub>2</sub> reaction over the Rh<sub>6</sub>(CO)<sub>16</sub>/SiO<sub>2</sub> sample indicates that the surface is somewhat catalytically active at 293 K as shown in fig. 8 (b'). Meanwhile the surface has a 1864 cm<sup>-1</sup> band upon exposure to C<sub>2</sub>H<sub>4</sub> + H<sub>2</sub>, which is assigned to the Rh bridged carbonyl. In addition, the formation of ethane in gas phase was also observed under hydroformylation conditions with Rh<sub>6</sub>(CO)<sub>16</sub>/SiO<sub>2</sub> (fig. 5), which is indicative of ethylene hydrogenation competing with ethylene hydroformylation over active species. The catalytic activity comparison among the three Rh surfaces with different saturations in figs. 9 and 10 supports the above interpretation.

Finally, it is of interest to discuss the contribution of coordinated CO to the catalysis for hydroformylation. The carbonyls from both Rh<sub>6</sub>(CO)<sub>16</sub> and its derivative are not reactive with C<sub>2</sub>H<sub>4</sub> + H<sub>2</sub> at 293 K to result in propanal, whereas this reaction is extremely facile for the linear CO adsorbed on Rh<sup>0</sup>. This difference shows the weak ability to insert of coordinated CO with respect to adsorbed CO from the gas phase, which can be interpreted from the viewpoint of Rh–CO bond strength. For the Rh<sub>6</sub>(CO)<sub>16</sub> compound, the enthalpy of the Rh–CO bond is estimated to be 182 kJ mol<sup>-1</sup> from the study of Housecroft et al. [41]. However, the corresponding energy of CO adsorption on metallic Rh surface is about 132 kJ mol<sup>-1</sup> [42,43]. Hence, the CO adsorbed on Rh desorbs more easily than the coordinated CO in the Rh complex dissociates in any case.

In principle, the reactivities of coordinated and adsorbed CO with C<sub>2</sub>H<sub>4</sub> + H<sub>2</sub> at 293 K cannot represent their ability to insert at catalytic reaction temperatures.

But the Rh–CO bond in Rh<sub>6</sub>(CO)<sub>16</sub> can be stabilized by gaseous CO at higher temperatures, so that the carbonyl ligand does not dissociate under hydroformylation conditions. The catalytic inactivity of Rh<sub>6</sub>(CO)<sub>16</sub> and the increase in catalytic activity with increasing unsaturation on the metallic Rh surface confirm this. In contrast, the Rh<sup>0</sup>-adsorbed CO desorbs easily since catalytic ethylene hydroformylation proceeds fastest on the totally decarbonylated Rh catalysts. In this study, the results of stoichiometric and catalytic ethylene hydroformylation with surface Rh–CO species appear significant to account for the role of coordinated CO in the heterogeneous catalysis. Coordinatively saturated Rh carbonyls can yield active sites only when it is decarbonylated. The thoroughly decarbonylated Rh catalysts are most effective.

## 5. Conclusion

(1) The oxidation chemistry of Rh<sup>0</sup> on SiO<sub>2</sub> under CO can be translated by the oxidation of highly dispersed metallic Rh particles to isolated Rh<sup>+</sup> by surface OH<sup>-</sup>, which converts to Rh<sup>+</sup>(CO)<sub>2</sub> after adsorbing CO, irrespective of dissociative CO adsorption on Rh<sup>0</sup>.

(2) Under atmospheric pressure, ethylene hydroformylation and ethylene hydrogenation have been found to be structure sensitive and structure insensitive, respectively. These relations and in situ IR study show that Rh<sup>0</sup> is uniquely responsible for heterogeneous catalytic hydroformylation on Rh/SiO<sub>2</sub>.

(3) The linear CO adsorbed on Rh<sup>0</sup>/SiO<sub>2</sub> is very reactive in CO insertion leading to the formation of propanal from C<sub>2</sub>H<sub>4</sub> + H<sub>2</sub> at 293 K, whereas the coordinated CO in Rh<sub>6</sub>(CO)<sub>16</sub>/SiO<sub>2</sub> and its carbonyl derivative is not reactive. Rh<sub>6</sub>(CO)<sub>16</sub>/SiO<sub>2</sub> can well be thermally stabilized by CO under hydroformylation conditions. Rh<sub>6</sub>(CO)<sub>16</sub>/SiO<sub>2</sub> is catalytically inactive. The Rh<sub>6</sub>(CO)<sub>16</sub> system exhibits an increased catalytic activity with increasing coordinative unsaturation on the Rh surface by decarbonylation. The Rh–CO bond is proposed to have a similar stability and to be inactive for CO insertion. By combining the reactivities of surface CO species with C<sub>2</sub>H<sub>4</sub> + H<sub>2</sub> with the catalytic activities of these species, it is suggested that rhodium-catalyzed heterogeneous hydroformylation needs the Rh<sup>0</sup> surface to be as coordinatively unsaturated as possible.

## References

- [1] E. Mantovani, N. Palladino and A. Zanobi, *J. Mol. Catal.* 3 (1977/78) 285.
- [2] M. Ichikawa, *J. Catal.* 59 (1979) 67.
- [3] M.E. Davis, J. Schmitzer, J.A. Rossin, D. Taylor and B.E. Hanson, *J. Mol. Catal.* 39 (1987) 243.
- [4] L. Alvila, T.A. Pakkanen, T.T. Pakkanen and O. Krause, *J. Mol. Catal.* 71 (1992) 281.
- [5] M. Lenarda, R. Ganzerla, L. Storaro, A. Trovarelli, R. Zandoni and J. Kaspar, *J. Mol. Catal.* 72 (1992) 75.
- [6] L. Alvila, T.A. Pakkanen, T.T. Pakkanen and O. Krause, *J. Mol. Catal.* 75 (1992) 33.
- [7] M. Lenarda, R. Ganzerla, S. Enzo, L. Storaro and R. Zandoni, *J. Mol. Catal.* 80 (1993) 105.
- [8] W.M.H. Sachtler and M. Ichikawa, *J. Phys. Chem.* 90 (1986) 4752.
- [9] M. Ichikawa, *Proc. 5th Int. Symp. on Relations between Homogeneous and Heterogeneous Catalysis* (1986) p. 819.
- [10] Y. Konishi, M. Ichikawa and W.M.H. Sachtler, *J. Phys. Chem.* 91 (1987) 6286.
- [11] M. Ichikawa, *Polyhedron* 127 (1988) 2351.
- [12] Y. Izumi, K. Asakura and Y. Iwasawa, *J. Catal.* 127 (1991) 631.
- [13] S.S.C. Chuang and S.I. Pien, *J. Catal.* 135 (1992) 618.
- [14] N. Takahashi, A. Mijin, H. Suematsu, S. Shinohara and H. Matsuoka, *J. Catal.* 117 (1990) 348.
- [15] C. Dossi, A. Fusi, L. Garlaschelli, D. Roberto, R. Ugo and R. Psaro, *Catal. Lett.* 11 (1991) 335.
- [16] L. Huang, Y. Xu, G. Piao, A. Liu and W. Zhang, *Catal. Lett.* 23 (1994) 87.

- [17] P. Chini and S. Martinengo, *Inorg. Chim. Acta* 3 (1969) 315.
- [18] A. Theolier, A.K. Smith, M. Leconte, J.M. Basset, G.M. Zanderighi, R. Psaro and R. Ugo, *J. Organomet. Chem.* 191 (1980) 415.
- [19] Q. Xin, G.Z. Liang, H. Zhang and J. Bi, *Petrochemical Technology (China)* 81 (1980) 461.
- [20] S.E. Wanke and N.A. Dougharty, *J. Catal.* 24 (1972) 367.
- [21] J.M. Basset and R. Ugo, *Aspects of Homogeneous Catalysis*, Vol. 3, ed. R. Ugo, ch. 2.
- [22] J.L. Bilhou, V. Bilhou-Bougnol, W.F. Graydon, J.M. Basset, A.K. Smith, G.M. Zanderighi and R. Ugo, *J. Organomet. Chem.* 153 (1978) 73.
- [23] H.F.J. van 't Blik, J.B.A.D. van Zon, T. Huizinga, J.C. Vis, D.C. Koningsberger and R. Prins, *J. Phys. Chem.* 87 (1983) 2264.
- [24] M. Primet, *J. Chem. Soc. Faraday Trans.* 72 (1978) 2570.
- [25] P. Basu, D. Panayotov and J.T. Yates Jr., *J. Am. Chem. Soc.* 110 (1988) 2074.
- [26] P. Gelin, J.-F. Dutel and Y. Ben Taarit, *J. Chem. Soc. Chem. Commun.* (1990) 1746.
- [27] T.T.T. Wong, A.Y. Stakkeev and W.M.H. Sachtler, *J. Phys. Chem.* 96 (1992) 7733.
- [28] T.T.T. Wong, Z. Zhang and W.M.H. Sachtler, *Catal. Lett.* 4 (1990) 365.
- [29] A.V. Kiseler and V.I. Lygin, *Infrared Spectra of Surface Compounds* (Wiley, New York, 1975) p. 80.
- [30] S. Takasaki, F. Koga, S. Tanabe, A. Ueno and Y. Kotera, *J. Chem. Soc. Jpn.* (1984) 998.
- [31] V. Hardeveld and V. Montfoort, *Surf. Sci.* 4 (1964) 396.
- [32] J.R. Anderson, *Structure of Metallic Catalysts* (Academic Press, New York, 1975).
- [33] G.A. Somorjai, *Catal. Lett.* 7 (1990) 169.
- [34] B.E. Koel, B.E. Bent and G.A. Somorjai, *Surf. Sci.* 146 (1984) 211.
- [35] E.K. Poels, *Faraday Discussions Chem. Soc.* 72 (1981) 194.
- [36] P.R. Watson and G.A. Somorjai, *J. Catal.* 74 (1982) 282.
- [37] J.M. Driessen, E.K. Poels, J.P. Hindermann and V. Ponc, *J. Catal.* 82 (1983) 26.
- [38] M. Kawai, M. Uda and M. Ichikawa, *J. Phys. Chem.* 89 (1985) 1654.
- [39] H. Arakawa, N. Takahashi, T. Hanaoka, K. Takeuchi, T. Matsuzaki and Y. Sugi, *Shokubai* 30 (1988) 492.
- [40] E.J. Rode, M.E. Davis and B.E. Hanson, *J. Catal.* 96 (1985) 574.
- [41] C.E. Housecroft, M.E. O'Neill, K. Wade and B.S. Smith, *J. Organomet. Chem.* 213 (1981) 35.
- [42] D.G. Castner, B.A. Sexton and G.A. Somorjai, *Surf. Sci.* 71 (1978) 519.
- [43] P.A. Thiel, E.D. Williams, J.T. Yates Jr. and W.H. Weinberg, *Surf. Sci.* 84 (1979) 54.